Video Article

Microfluidic Mixers for Studying Protein Folding

Steven A. Waldauer[1], Ling Wu[1], Shuhuai Yao[2], Olgica Bakajin[3], Lisa J. Lapidus[1]

[1]Department of Physics and Astronomy, Michigan State University

[2]Department of Mechanical Engineering, Hong Kong University of Science and Technology

[3]Center for Biophotonics, University of California, Davis

Correspondence to: Lisa J. Lapidus at lapidus@msu.edu

URL: http://www.jove.com/video/3976
DOI: doi:10.3791/3976

Keywords: Bioengineering, Issue 62, microfluidic mixing, laminar flow, protein folding, fluorescence, FRET

Date Published: 4/10/2012

Citation: Waldauer, S.A., Wu, L., Yao, S., Bakajin, O., Lapidus, L.J. Microfluidic Mixers for Studying Protein Folding. *J. Vis. Exp.* (62), e3976, doi:10.3791/3976 (2012).

Abstract

The process by which a protein folds into its native conformation is highly relevant to biology and human health yet still poorly understood. One reason for this is that folding takes place over a wide range of timescales, from nanoseconds to seconds or longer, depending on the protein[1]. Conventional stopped-flow mixers have allowed measurement of folding kinetics starting at about 1 ms. We have recently developed a microfluidic mixer that dilutes denaturant ~100-fold in ~8 μs[2]. Unlike a stopped-flow mixer, this mixer operates in the laminar flow regime in which turbulence does not occur. The absence of turbulence allows precise numeric simulation of all flows within the mixer with excellent agreement to experiment[3-4].

Laminar flow is achieved for Reynolds numbers *Re* ≤100. For aqueous solutions, this requires micron scale geometries. We use a hard substrate, such as silicon or fused silica, to make channels 5-10 μm wide and 10 μm deep (See **Figure 1**). The smallest dimensions, at the entrance to the mixing region, are on the order of 1 μm in size. The chip is sealed with a thin glass or fused silica coverslip for optical access. Typical total linear flow rates are ~1 m/s, yielding *Re*~10, but the protein consumption is only ~0.5 nL/s or 1.8 μL/hr. Protein concentration depends on the detection method: For tryptophan fluorescence the typical concentration is 100 μM (for 1 Trp/protein) and for FRET the typical concentration is ~100 nM.

The folding process is initiated by rapid dilution of denaturant from 6 M to 0.06 M guanidine hydrochloride. The protein in high denaturant flows down a central channel and is met on either side at the mixing region by buffer without denaturant moving ~100 times faster (see **Figure 2**). This geometry causes rapid constriction of the protein flow into a narrow jet ~100 nm wide. Diffusion of the light denaturant molecules is very rapid, while diffusion of the heavy protein molecules is much slower, diffusing less than 1 μm in 1 ms. The difference in diffusion constant of the denaturant and the protein results in rapid dilution of the denaturant from the protein stream, reducing the effective concentration of the denaturant around the protein. The protein jet flows at a constant rate down the observation channel and fluorescence of the protein during folding can be observed using a scanning confocal microscope[5].

Video Link

The video component of this article can be found at http://www.jove.com/video/3976/

Protocol

1. Fabrication of Microfluidic Mixing Chips

Figure 3 shows the basic fabrication steps.

1. Clean 4 inch (100 mm) fused silica wafers with fresh Piranha solution (3:1 H_2SO_4:H_2O_2): i) Heat the sulfuric acid to 130 °C then pour in the peroxide. Note that the surface roughness and the flatness of the fused silica wafers used play an important role for the final bonding step. ii) Immerse the wafers for at least 30 minutes. iii) Rinse for 5 minutes with water and dry. Apply a polysilicon (poly) coating, ~1 μm thick per every intended 10 μm depth of the final microfluidic channels, using a low pressure chemical vapor deposition (LPCVD) furnace.
2. Clean the wafers and mask using the Piranha protocol in step 1.1. Clean the mask the same way, then rinse with acetone, methanol and isopropanol and blow dry immediately. Dehydrate the wafers on a hot plate at 150 °C for ~10 minutes (use an aluminum foil tent to keep particulates away) or in a 120 °C oven for at least 120 min (overnight preferably). To increase photoresist adhesion, immediately expose the warm wafers to HMDS vapor for 5 minutes. Spin coat the wafers with a ~900 nm thick layer of AZ5214 photoresist and soft bake at 90 °C directly on a hotplate for 1 minute or in an oven at 110 °C for 30 min (**Figure 3**, step 1).
3. Align the mask and make a hard and vacuum contact. Expose to UV light for several seconds (total energy: ~103 mJ/cm^2) (**Figure 3**, step 2). Develop with AZ400K developer, diluted 4:1 with DI water for ~50 seconds (until photoresist is fully developed) while gently agitating. Rinse with water for 2 minutes. Inspect features with microscope (**Figure 3**, step 3). If features are poorly resolved, strip the photoresist and start again from 1.2. Hard bake 115 °C directly on a hotplate for 2 minutes.

4. Descum wafers with Asher or O_2 plasma for 2.5 minutes at 100 W RF power. Using a deep reactive ion etcher (DRIE), etch the polysilicon layer all the way through to the fused silica below. Strip the remaining photoresist with PRS2000 resist stripper at 75 °C for 10 minutes. Rinse and dry. Measure the etch depth to ensure it is all the way through the poly coating (**Figure 3**, step 4).
5. Using an oxide capable DRIE such as an ULVAC NLD-6000 etcher, etch fused silica to a depth of ~10 µm per micron thickness of the poly coating (**Figure 3**, step 5). This poly coating will be worn away during etching, so it may be necessary to check on the integrity of the coating periodically during the etching process. If intentionally featureless regions of the wafer surface have become stripped bare of the protective poly coating during etching, the surface has most likely become pitted and will no longer be suitable for bonding in the final steps of production. In this case the wafer is most likely no longer viable. Clean with the Matrix Asher for 4 minutes, 100 W RF power. Strip the polysilicon with a XeF_2 etcher (**Figure 3**, step 6). It may be necessary to repeat step 1.4 and this step a few times to remove all of the photoresist and poly coatings.
6. Spin coat wafers with a new ~1 µm layer of photoresist to protect the channels during subsequent handling. Drill entrance and exit holes in each chip using a computer controlled diamond-tipped drill or manually with a sandblaster (**Figure 3**, step 7). If using a drill, mount the wafer (feature-side down) on a sacrificial glass plate using Aqua Bond 55, taking care to keep the bonder free of bubbles. Cool the drill with micro-90 cleaning solution. This keeps small bits of glass from sticking to the channels which then clog the chip during use.
7. Rinse the wafer with DI water using a syringe to inject water into each hole. Soak in soapy water for an hour. Remove photoresist and Aqua Bond with PRS 2000 at 60 °C for several hours until surface is clean. Rinse wafer with DI water and warm soapy water. Rinse each hole again with a syringe, avoiding etched features. Dry wafer with nitrogen and in a vacuum oven set to 120 °C. Inspect holes to ensure they are free of grit and repeat cleaning steps as necessary. Measure the depth of the channels with either an optical or mechanical surface profiler (**Figure 3**, step 8).
8. Clean wafers and an equivalent number of 170 µm thick fused silica cover glasses with 1) Piranha solution (1-2 hours according to the procedure in 1.1), 2) RCA 2 (5:1:1 DI:HCl:H_20_2) solution for 10 minutes at 75 C, 3) RCA 1 solution (5:1:1 DI:NH_4OH:H_20_2) for 22 minutes at 75C). Rinse with DI water for 5 minutes between each solution.
9. Place one wafer features side up on top of a stack of 3-4 cleanroom wipes placed on top of a hard flat surface, such as a small pane of glass. Dry the wafer thoroughly with nitrogen gas for at least 5 minutes. Repeat with cover glass. Pick up cover glass by the edge and invert such that the polished side is face down held over the wafer and align the flat edges. Carefully drop the cover glass onto the wafer and allow it to settle. Nudge horizontally only to adjust alignment. Push down with one finger on the center of the wafer. One should see a bonding front begin to radiate outward. If necessary, apply additional pressure to other positions around the wafer to advance the bonding front (**Figure 3**, step 9).
10. Place the sealed wafers in a high temperature oven set to ramp from room temp to 800 °C over 3 hours, then from 800 - 1100 °C over another 1.2 hours. Hold at 1100 °C for 2 hours, and then ramp down to room temperature over another 1.5 hours.
11. Dice with a wafer dicing saw into individual chips (**Figure 3**, step 10).
12. The protocol describes the fabrication of channels in the fairly unusual fused silica substrate which is necessary for UV detection. But this protocol can also be adapted for a silicon substrate which requires only one etching step[2]. A glass (but not fused silica) cover glass can be bonded to the wafer using anodic bonding.

2. Mounting and Loading Chips

1. The manifold to hold the mixing chip and solutions can be made of plastic, such as Lexan or Plexiglas , or aluminum for temperature control (see **Figure 4**). If using aluminum, the solution reservoirs should be coated with parylene to prevent the dissolution of aluminum by the salt solutions in the reservoirs. The temperature of the entire manifold, solutions and chip can be controlled with thermoelectric devices mounted on the sides and an electronic controller.
2. The chip is mated to the manifold by small o-rings and a held in place with a retaining ring that allows a clear optical view of the center of the chip. The o-ring grooves should be shallower than standard to ensure good mating without applying too much pressure to the chip, i.e., a 002 o-ring should be 0.025" deep. Once the chip is mounted, add solutions to the center and side reservoirs, taking care to release any bubbles trapped at the bottom of the wells.
3. Because the volumes used in this mixer are so small, the flow can be controlled with air pressure applied above the solution wells. **Figure 4** shows the pressure manifold mated to the top of the chip manifold by o-rings. The pressure manifold is connected to computer-controlled pressure transducers that can maintain pressures from ~2-80 PSI. The chip has been designed such that equal pressures on the center and side channels produce a ~100-fold ratio in the linear flow rates. At 20 PSI, the linear flow rate in the exit channel is ~1 m/s.
4. Place manifold on an inverted microscope and examine mixing region with the eyepiece or camera output. An incandescent flashlight placed on top of the manifold will provide enough light. Use a dye or high index of refraction solution (i.e. 6 M guanidine hydrochloride) in the center channel to view of the jet.
5. At equal pressure on the center and side channels, the jet will be difficult to see by eye so start with the side channel pressure at 0 PSI and slowly increase to equal pressure. If one side channel is clogged, the jet will be pushed against one of the walls of the exit channel. If a visible clog appears, it may be dislodged by applying pressure or vacuum to the exit channel with a syringe.
6. If protein or other organic material clogs the chip, it can be cleaned by soaking in Pirhana solution overnight.

3. Data Collection

Figure 5 shows the basic optical instrument layout.

1. Bring a collimated laser beam into a research-grade microscope using a dichroic mirror either inside or just outside the microscope. Align the laser so that the focus can be seen in the eyepiece or camera somewhat near the mixing region.
2. Fluorescence from the protein in the mixer is collected by the objective and sent through the dichroic mirror, focused by a lens to a pinhole and imaged on a photon counter. Scan the chip using a piezoelectric scanner in x and y to image the mixing region (typical step size is 2 µm). Choose a position on the jet and scan in x and z to find the focus at the center of the channel vertically. The depth of field of the microscope is much less than the channel depth and the flow rate is uniform in the channel except within 1 µm of the walls. Therefore the temporal resolution of the observed fluorescence is determined primarily by the size of the confocal spot.

3. Scan horizontally within the exit channel (typical step size is 0.2 μm in across the jet, 2 μm along the jet) in 100 μm increments along the jet, observing for ~1 ms per position (see **Figure 6**). Move the microscope stage by 80-90 μm along the jet to capture later times.
4. Alternatively, light can be detected by a spectrograph and CCD after the dichroic mirror using a lens to focus the light onto the entrance slit. Since data collection is slower than for the photon counter (1 second per position), typically the jet is imaged first with the photon counter and then points along the jet are measured with the spectrograph (see **Figure 7**).
5. Data from the photon counter is analyzed by summing 3-5 pixels around the jet at each position to create a plot of intensity vs. distance. Time is calculated from distance using a calculated velocity based on the applied pressures (see **Figure 8**).
6. Data from the spectrograph can be analyzed a couple of ways. For FRET, channels designated as "donor" and "acceptor" can each be summed and the proximity ratio $E=I_A/(I_D+I_D)$ calculated (see **Figure 9**). Alternatively, single value decomposition can be performed to look at independent spectral components vs. time, such as the shift in the tryptophan emission spectrum as a protein folds.
7. Distance within the exit channel can be converted to time using the constant flow rate determined from the applied pressure to the side channels. Within the first 2 μm of the exit channel, the flow rate of the protein jet accelerates ~100x and the times in that region must be calculated with finite element analysis of the streamlines (producing the times plotted in **Figure 8**). This acceleration produces an offset of ~1-2 μs after the velocity becomes constant and can usually be ignored in measuring kinetics much slower than mixing.

4. Representative Results

Figure 6 shows a contour plot of the intensity in the mixing region measured by the photon counter. The background in the exit channel outside of the jet should be close to the noise floor of the detector and is typically not subtracted. A higher background may indicate poor alignment or that the protein is sticking to the walls of the channel. A jet that looks kinked or crooked, especially near the mixing region, indicates a poor etch of the nozzles.

Figure 7 shows the time resolved spectra from the protein acyl-coenzyme A-binding protein (ACBP) labeled with Alexa 488 and Alexa 647. This data has been background subtracted to remove the dark charge and laser signal. The background signal was taken with the center channel pressure set to 0 PSI.

The mixing time can be measured by measuring a rapid reaction that is much faster than mixing such as Trp fluorescence quenching by KI or collapse of single stranded DNA, labeled with FRET dyes, by the addition of NaCl. Because the jet is smaller than the optical resolution of the microscope, there is a large intensity drop in the mixing region as the jet forms. This instrument response can be removed by making a control measurement in which no solution conditions change. **Figure 8** shows the ratio of mixing (into 400 mM KI) and non-mixing experiments of N-acetyl tryptophan amide fluorescence. The line shows the predicted concentration of KI from COMSOL simulations. The mixing time, as measured as the time for the concentration to decrease 80%, is 8 μs.

Since data is collected in 100 μm increments along the 500 μm-long exit channel, data must be pasted together from multiple views. There are occasionally small offsets in signal between these views, likely due to small changes in the focus as the chip is moved by the microscope stage. By moving the stage 80 or 90 μm per view, these offsets can be eliminated by examining overlapping data. Typically data is collected with at least two flow rates and the data is combined to confirm any signal changes are due to real spectroscopic changes in the protein, rather than optical or flow effects. **Figure 9** shows the FRET changes in the protein ACBP after dilution of denaturant from 6 M to 0.06 M. This data does not need a control experiment since the FRET is already a ratio and the instrument response is already removed. The rapid jump near T=0 represents a rapid change in FRET signal within the mixing time.

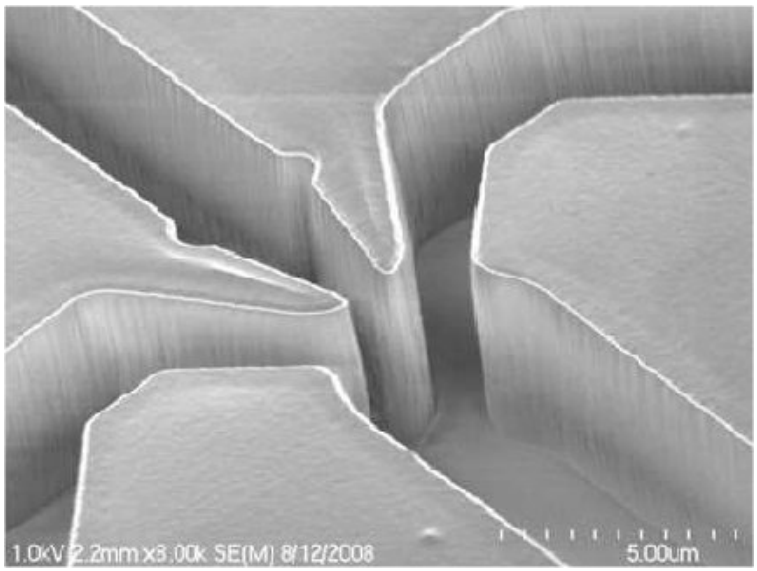

Figure 1. Layout of mixing region measured by electron microscopy.

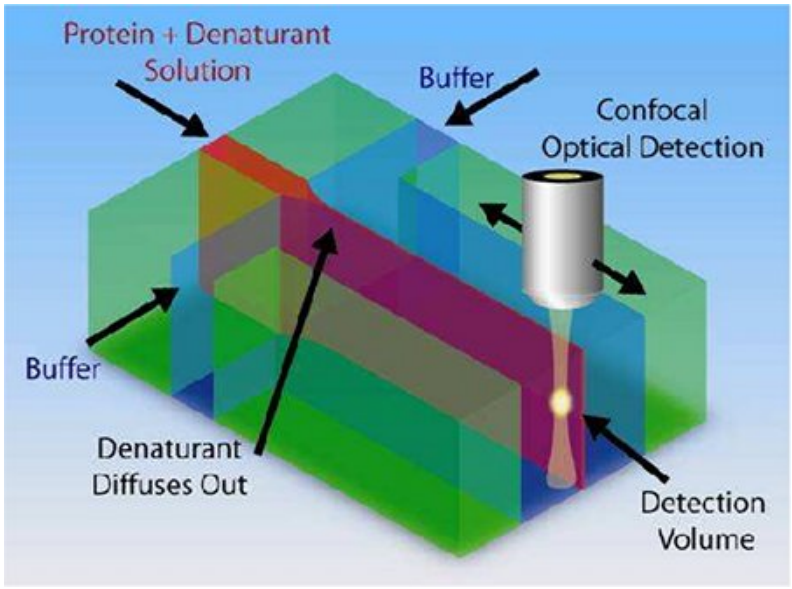

Figure 2. Schematic of hydrodynamic mixing to study protein folding. The protein, dissolved in high denaturant to unfold it, flows down the center channel towards the mixing region where it meets buffer flowing ~100 times faster. Laminar flow forces the protein stream into a narrow jet from which denaturant molecules can rapidly diffuse. As the jet flows down the exit channel, the protein can be observed with high spatial and time resolution using a confocal microscope.

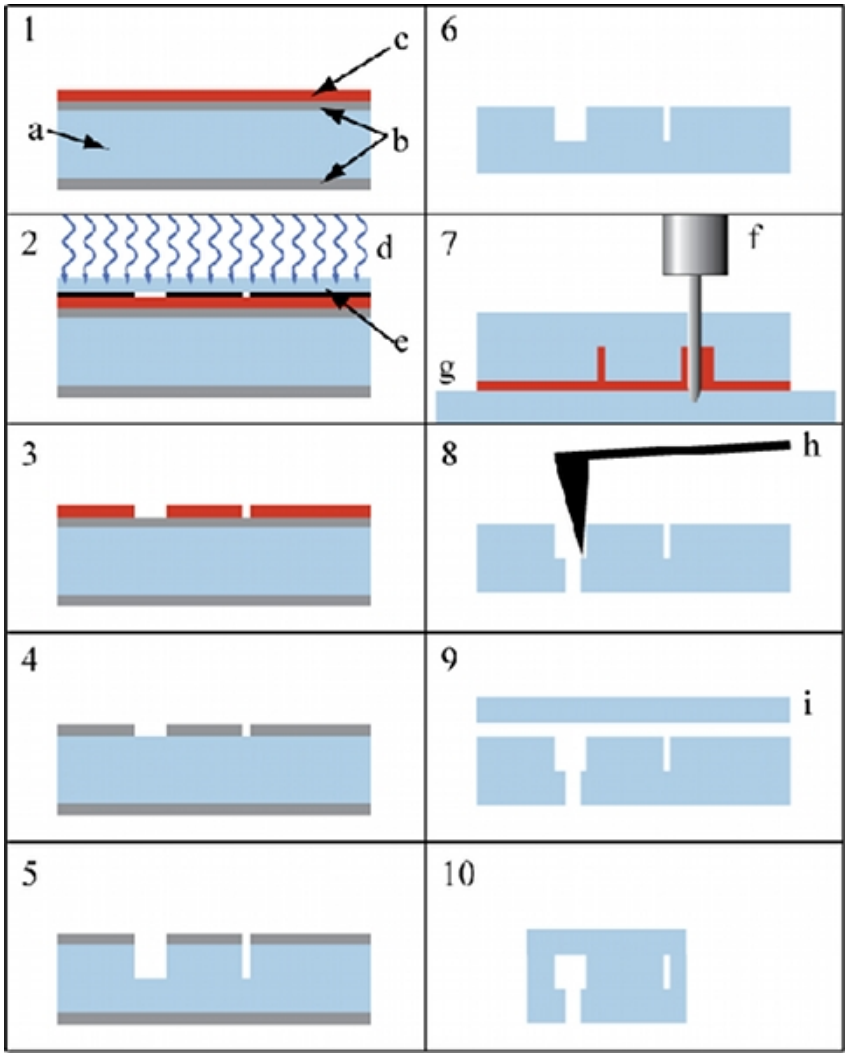

Figure 3. Fused silica fabrication. 1) The process starts with a highly polished 500 µm thick fused silica substrate (a) with a layer of polysilicon (poly) deposited on the top and bottom surfaces (b) and spin-coated with a layer of photoresist (c). 2) A photomask (e) is brought into hard contact with the wafer and the photoresist is exposed to UV light (d). 3) The wafer is placed in a developer bath and the pattern is revealed in the photoresist. 4) The wafer is placed in a DRIE and the features are etched into the top poly coating. The photoresist is then removed. 5) The poly then acts as a mask when the wafer is placed in an oxide etcher and the features are etched 10 - 40 µm into the fused silica substrate. 6) The poly coating is then removed in a XeF_2 etcher. 7) The wafer is bonded to a sacrificial glass plate with a heat-activated sealant (g), features side down, and a diamond drill bit (f) abrasively drills through-holes from the backside. 8) A surface profiler (h) then directly measures the etched feature depths. 9) A 170 µm thick fused silica coverslip wafer is directly bonded on the top surface of the wafer. 10) The wafer is diced into individual microfluidic chips.

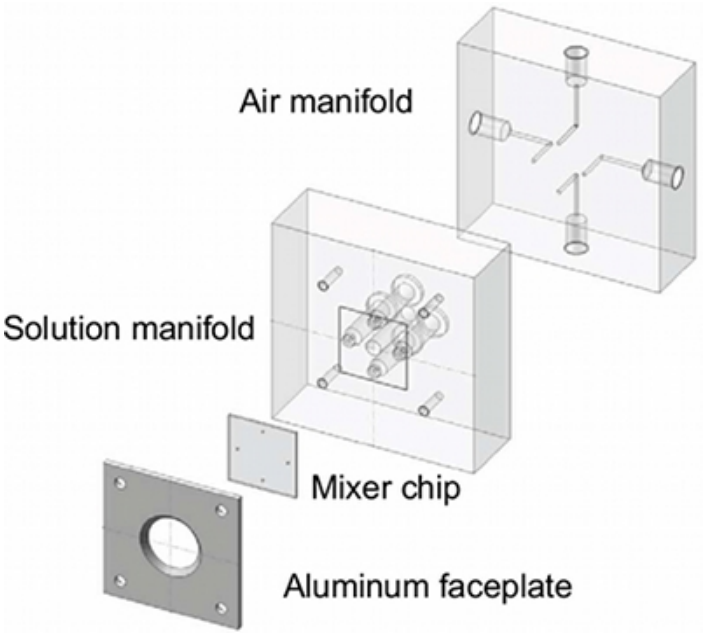

Figure 4. The mixer manifold. The microfluidic-chip is secured to the solution manifold with a machined aluminum faceplate and four o-rings under the ~200 µL reservoirs. A large hole is machined through the center of the manifold directly above the mixing region of the affixed microfluidic-chip, allowing excess UV light to escape without backscattering, inhibiting any auto-fluorescence from the manifold itself and allowing direct illumination of the chip by eye or camera for alignment. The air manifold seals each of the reservoirs such that the air pressure in each can be controlled via an external pressure control box.

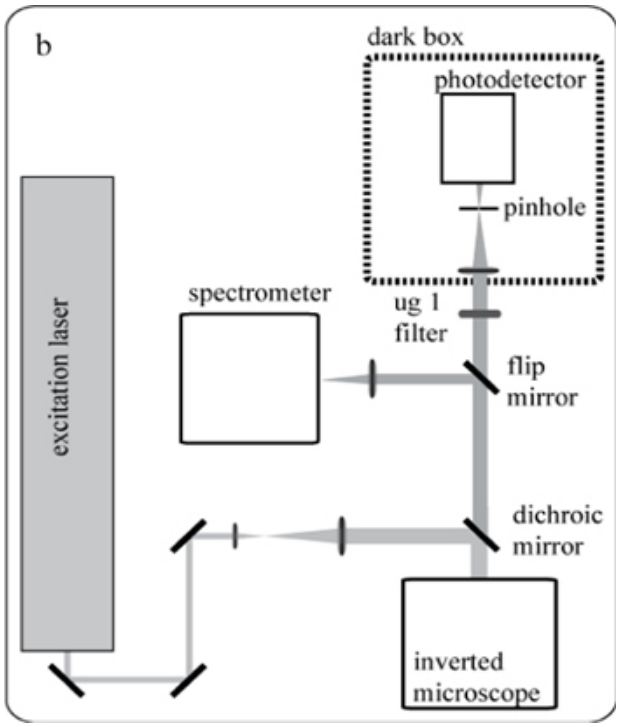

Figure 5. Schematic of optical confocal microscope.

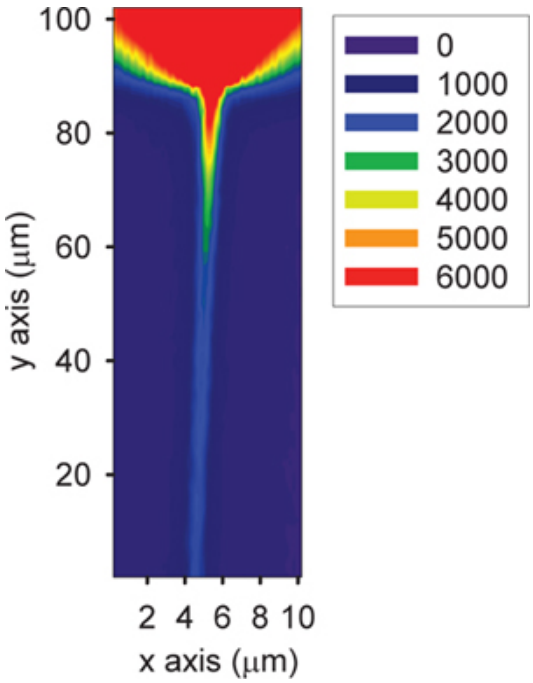

Figure 6. Contour plot of tryptophan fluorescence in the microfluidic mixer. The mixing region is located at ~90 μm on the y-axis.

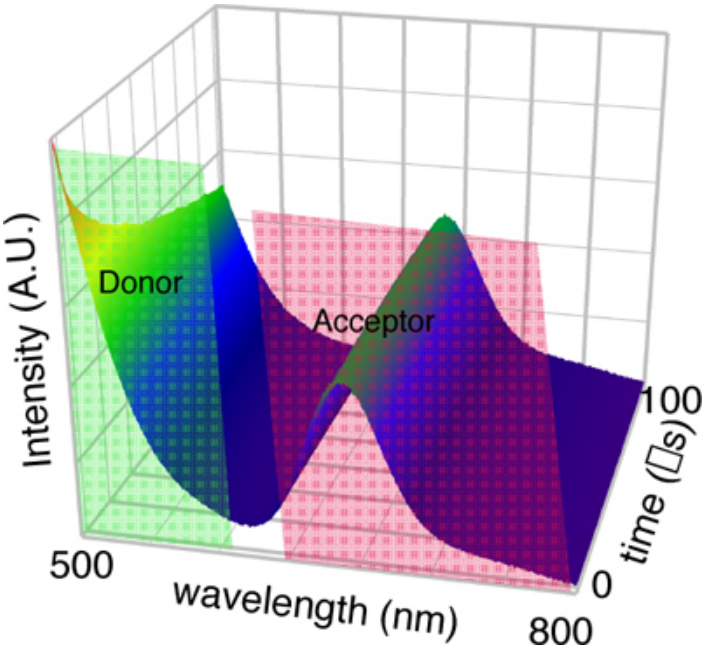

Figure 7. Time dependent fluorescent spectra collected within the mixer. The green and red rectangles show the wavelengths designated as donor and acceptor channels, respectively.

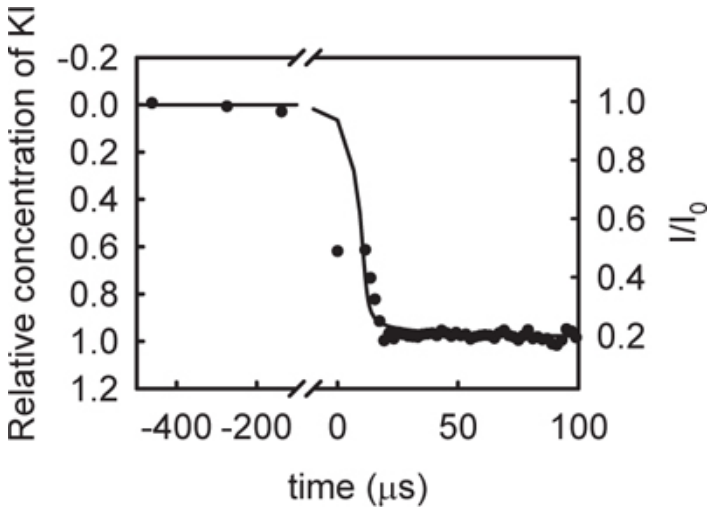

Figure 8. Mixing time measured by fluorescence quenching of tryptophan by potassium iodide (points and right axis) and calculated by finite element analysis (line and left axis).

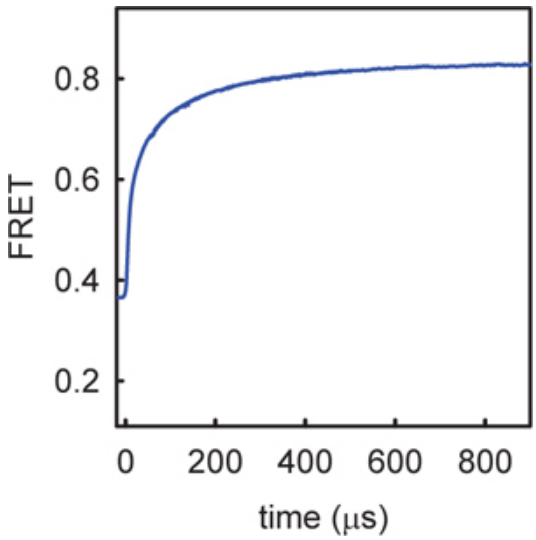

Figure 9. FRET changes measured during the folding of the protein ACBP. The rapid rise near t=0 represents a burst phase within the mixing time and the slower rise represents a gradual accumulation of structure as the protein folds. The data was taken at two different flow rates and overlaid, leading to different densities of measurements at different times.

Discussion

Rapid mixing has been a development goal for the field of protein folding for many years because it has long been recognized that molecular processes of biomolecules occur over time scales ranging from picoseconds to seconds. Conventional stopped-flow mixers have dead times of 1-5 ms which is primarily limited by turbulence. Turbulent continuous flow mixers with mixing times of 30-300 μs have been developed over the past 15 years by a small number of groups but generally require high flow rates to achieve these mixing times and therefore use a lot of sample[6-8].

This protocol describes the use of microfluidic mixing chips to achieve rapid dilution in the laminar flow regime. There are multiple advantages to working within this regime, but a primary one is the ability to simulate the entire mixing process with high precision which allows one to modify the mixing response. T-mixers developed by other groups with simple geometries have demonstrated mixing times of 100-200 μs that were primarily limited by the size of the channels[9-10]. By scaling the size of the channels to 10 μm Knight reduced the mixing time to ~10 μs[11]. Yao and Bakajin showed that small changes in geometry could lead to significant improvements in the mixing time[4]. However, that work showed that acceleration of mixing can also lead to slower phases as well. The design used in this work[12-13] is a compromise between the two best designs in reference[4] to minimize the slower exponential decay in denaturant concentration and also to make the feature more reproducible in DRIE etching.

There has been some controversy in the field of ultrarapid mixing over the definition of the mixing time. It is important to recognize the difference between "mixing time" and "dead time". The dead time is defined in a turbulent mixer as the time during which a measurement cannot be made and may in fact be significantly longer than the actual mixing time. It is typically determined by making several measurements of a pseudo-first order bimolecular reaction (such as quenching of tryptophan fluorescence by N bromosuccinate) at various concentrations. The observed

exponential decays are fitted to converge at a single value assumed to be t=0 s and the time between that point and the first measured point is the dead time. For laminar flow mixers, measurements can be made during the mixing process so there is no dead time, only a mixing time. The mixing time is simply the time to combine two solutions until sufficient uniformity is reached. We have previously defined the mixing time to be a 90/10 time, the time for the concentration of denaturant to decrease from 90% to 10% of the unmixed value. However, the shape of the mixing curve is not perfectly symmetric with the tail of the decay having a small exponential component. Furthermore, protein folding has a highly non-linear dependence on denaturant concentration so that folding can often commence even if the denaturant is only reduced by two fold. Therefore we have more recently defined the mixing time as the time to reduce the denaturant concentration by 80%. Certainly other definitions can be used depending on the requirements of the experiment.

The use of this mixer to study protein folding has consistently revealed surprising results. Folding of cytochrome c and apomyoglobin have long been studied to have multiple folding steps and early results with continuous flow mixers showed collapse to occur on the ~100 μs timescale[10,14-15]. Our measurements with this mixer showed there to be at least 2 steps on this timescale, a very fast, likely non-specific, collapse (as measured by Trp fluorescence spectral shift) within the mixing time of the mixer followed by a slower phase (as measured by the quenching of total Trp emission) that is likely the first formation of native structure[5]. We have also observed a 50 μs process in the B1 domain of protein L, overturning the conventional interpretation that this protein is a 2-state folder[13].

An advantage of this rapid mixer is that it can probe the folding of the fastest folding proteins that have usually only been measureable by nanosecond T-jump instruments. T-jump typically requires observation of folding/unfolding relaxation near the melting temperature of the protein and therefore never follows the folding of the entire population. With this mixer we have looked at the folding of γ-repressor (λ^{6-86}) with both Trp total emission and spectral shift and have found evidence that the protein has no barrier to folding under strong folding conditions that were not accessible to previous T-jump measurements[12]. Finally we have measured the folding of the villin headpiece HP-35, one of the fastest folders yet measured and found that the folding rate measured after mixing is ~5 times slower than measured by T-jump under the same conditions[16]. This suggests that folding kinetics depends on the starting conditions, overturning a major assumption in the field.

Disclosures

We have nothing to disclose.

Acknowledgements

This work is supported by National Science Foundation FIBR (NSF EF-0623664) and IDBR (NSF DBI-0754570). This work was partially supported by funding from National Science Foundation FIBR Grant 0623664 administered by the Center for Biophotonics, an NSF Science and Technology Center, managed by the University of California, Davis, under Cooperative Agreement PHY 0120999. The research of Lisa Lapidus, Ph.D. is supported in part by a Career Award at the Scientific Interface from the Burroughs Welcome Fund.

References

1. Eaton, W.A., *et al.* Fast kinetics and mechanisms in protein folding. *Annual Review of Biophysics and Biomolecular Structure.* **29**, 327-359 (2000).
2. Hertzog, D.E., *et al.* Femtomole mixer for microsecond kinetic studies of protein folding. *Analytical Chemistry.* **76**, 7169-7178 (2004).
3. Hertzog, D.E., Ivorra, B., Mohammadi, B., Bakajin, O., & Santiago, J.G. Optimization of a microfluidic mixer for studying protein folding kinetics. *Analytical Chemistry.* **78**, 4299-4306 (2006).
4. Yao, S. & Bakajin, O. Improvements in Mixing Time and Mixing Uniformity in Devices Designed for Studies of Protein Folding Kinetics. *Analytical Chemistry.* **79**, 5753-5759 (2007).
5. Lapidus, L.J., *et al*. Protein Hydrophobic Collapse and Early Folding Steps Observed in a Microfluidic Mixer. *Biophysical Journal.* **93**, 218-224 (2007).
6. Bilsel, O., Kayatekin, C., Wallace, L.A., & Matthews, C.R.A microchannel solution mixer for studying microsecond protein folding reactions. *Review of Scientific Instruments.* **76**, (2005).
7. Chan, C.-K., *et al*. Submillisecond protein folding kinetics studied by ultrarapid mixing. *PNAS.* **94**, 1779-1784 (1997).
8. Shastry, M.C.R., Luck, S.D., & Roder, H. A continuous-flow capillary mixing method to monitor reactions on the microsecond time scale. *Biophysical Journal.* **74**, 2714-2721 (1998).
9. Pollack, L., *et al*. Compactness of the denatured state of a fast-folding protein measured by submillisecond small-angle x-ray scattering. *Proceedings of the National Academy of Sciences of the United States of America.* **96**, 10115-10117 (1999).
10. Takahashi, S., *et al.* Folding of cytochrome c initiated by submillisecond mixing. *Nature Structural Molecular Biology.* **4**, 44-50 (1997).
11. Knight, J.B., Vishwanath, A., Brody, J.P., & Austin, R.H. Hydrodynamic focusing on a silicon chip: Mixing nanoliters in microseconds. *Physical Review Letters.* **80**, 3863-3866 (1998).
12. DeCamp, S.J., Naganathan, A.N., Waldauer, S.A., Bakajin, O., & Lapidus, L.J. Direct Observation of Downhill Folding of lambda-Repressor in a Microfluidic Mixer. *Biophysical Journal.* **97**, 1772-1777 (2009).
13. Waldauer, S.A., *et al.* Ruggedness in the folding landscape of protein L. *Hfsp Journal.* **2**, 388-395 (2008).
14. Shastry, M.C.R. & Roder, H. Evidence for barrier-limited protein folding kinetics on the microsecond time scale. *Nature Structural Biology.* **5**, 385-392 (1998).
15. Uzawa, T., *et al.* Collapse and search dynamics of apomyoglobin folding revealed by submillisecond observations of alpha-helical content and compactness. *Proceedings of the National Academy of Sciences of the United States of America.* **101**, 1171-1176 (2004).
16. Zhu, L., *et al.* Evidence of Multiple Folding Pathways for the Villin Headpiece Subdomain. *The Journal of Physical Chemistry B.* **115**, 12632-12637 (2011).